

A EUROPEAN JOURNAL

# CHEMPHYSICHEM

OF CHEMICAL PHYSICS AND PHYSICAL CHEMISTRY

## Accepted Article

**Title:** Effect of the solvent choice in the self-assembly properties in a diphenylalanine amphiphile stabilized by an ion pair

**Authors:** Enric Mayans, Gema Ballano, Javier Sendros, Merçe Font-Bardia, J. Lourdes Campos, Jordi Puiggali, Carlos Cativiela, and Carlos Aleman

This manuscript has been accepted after peer review and appears as an Accepted Article online prior to editing, proofing, and formal publication of the final Version of Record (VoR). This work is currently citable by using the Digital Object Identifier (DOI) given below. The VoR will be published online in Early View as soon as possible and may be different to this Accepted Article as a result of editing. Readers should obtain the VoR from the journal website shown below when it is published to ensure accuracy of information. The authors are responsible for the content of this Accepted Article.

**To be cited as:** *ChemPhysChem* 10.1002/cphc.201700180

**Link to VoR:** <http://dx.doi.org/10.1002/cphc.201700180>

WILEY-VCH

[www.chemphyschem.org](http://www.chemphyschem.org)

A Journal of



# Effect of the solvent choice in the self-assembly properties in a diphenylalanine amphiphile stabilized by an ion pair

Enric Mayans,<sup>[a,b]</sup> Gema Ballano,<sup>[c]</sup> Javier Sendros,<sup>[a,b]</sup> Merçè Font-Bardia,<sup>[d,e]</sup> J. Lourdes Campos,<sup>[a]</sup> Jordi Puiggali,<sup>\*[a,b]</sup> Carlos Cativiela,<sup>\*[c]</sup> and Carlos Alemán<sup>\*[a,b]</sup>

**Abstract:** A diphenylalanine amphiphile blocked at the C-terminus with a benzyl ester and stabilized at the N-terminus with a trifluoroacetate (TFA) anion has been synthesized and characterized. The aggregation of peptide molecules has been studied considering a peptide solution in an organic solvent and adding pure water, a KCl solution or another organic solvent as co-solvent. The choice of the organic solvent and co-solvent, and the solvent:co-solvent ratio allows tuning the mixture by modulating the polarity, the ionic strength and the peptide concentration. Differences in the properties of the media used to dissolve the peptides result in the formation of different self-assembled microstructures (e.g. fibers, branched-like structures, plates and spherulites). Furthermore, crystals of TFA-FF-OBzl have been obtained for X-ray diffraction from aqueous peptide solutions. Results reveal a hydrophilic core constituted by carboxylate (from TFA), ester and amide groups, which is surrounded by a hydrophobic crown with ten aromatic rings. This segregated organization explains the assemblies observed in different solvent mixtures as a function of the environmental polarity, ionic strength and peptide concentration.

## Introduction

In their pioneering work, Reches and Gazit<sup>[1]</sup> demonstrated the

formation of diphenylalanine (FF, where F= L-Phe) nanotubes in aqueous solution, which is due to the directionality offered by a combination of hydrogen bonding and repeated phenyl stacking interactions. In subsequent studies the FF was proved as a minimal sequence that forms self-assembled peptide nanostructures,<sup>[2–8]</sup> giving place to the development of a new class of biomaterials that is based on the addition of various N- and C-terminal capping groups to the aromatic FF or, even, on chemical modification of the own F residues.

The peptide amphiphile Fmoc-FF (Fmoc= fluorenylmethoxycarbonyl), which form stable gels, is among the most studied FF-based biomaterials. Thus, Fmoc-FF gels with a variety of properties have been prepared using different approaches.<sup>[9]</sup> Gazit and co-workers formed gels by dissolving Fmoc-FF in an appropriate water-miscible solvent,<sup>[10,11]</sup> while Ulijn and co-workers used a pH switch approach coupled with changes in the temperature to yield Fmoc-FF gels with variable properties (*i.e.* depending on the rate of pH decrease and the final pH).<sup>[12–15]</sup> The mixing method was also used by other groups, showing that the mechanical properties of Fmoc-FF gels depend on the final ratio of dimethylsulfoxide (DMSO) to water.<sup>[16,17]</sup> More recently, Adams and co-workers formed Fmoc-FF gels by dissolving the peptide in an organic solvent (OS) and adding water, rheological properties depending on the choice of the OS.<sup>[18]</sup> Furthermore, gels formed using acetone were metastable and single crystals suitable for X-ray diffraction were collected. The structure showed a parallel stacking of Fmoc-FF molecules, neighbouring molecules interacting through hydrogen bonds and weak offset  $\pi$ - $\pi$  interactions.<sup>[18]</sup> Similarly, studies on Nap-FF (Nap= naphthalene) and Cbz-FF (Cbz= benzylloxycarbonyl) hydrogels evidenced fibrous structures made of  $\beta$ -sheet arrangements, even though fibril dimensions depended on the aromatic capping group.<sup>[19]</sup> Interestingly, the Fmoc-FF-OFm peptide, capped with Fmoc and 9-fluorenylmethyl ester (OFm) at the N- and C-terminal, respectively, exhibited a great variety of polymorphic microstructures (*e.g.* doughnut, stacked-braids, dendritic and microtubes) depending on the solvents used to promote the self-assembly.<sup>[20]</sup> It is worth noting that stacking interactions play a dominant role in such highly aromatic peptide.

An alternative approach is the chemical modification of the F residues. Reches and Gazit<sup>[5]</sup> explored the self-assembly of FF-based dipeptides in which the phenyl side chains were modified by halogen atoms, additional phenyl groups or with nitro substitutions. These homo-aromatic dipeptide motifs formed tubular, spherical and fibrillary structures in the nanoscale, in some cases nanocrystals and 2D nanoplates being also detected. These results proved that the properties of FF-based biomaterials can be properly tailored by engineering the F residue.

[a] E. Mayans, J. Sendros, Dr. J. L. Campos, Prof. Dr. J. Puiggali and Prof. Dr. C. Alemán  
Departament d'Enginyeria Química  
Universitat Politècnica de Catalunya  
EEBE, Edifici I.2, C/ Eduard Maristany, 10-14, 08019, Barcelona, Spain  
E-mail: [jordi.puiggali@upc.edu](mailto:jordi.puiggali@upc.edu) and [carlos.aleman@upc.edu](mailto:carlos.aleman@upc.edu)

[b] E. Mayans, J. Sendros, Prof. Dr. J. Puiggali and Prof. Dr. C. Alemán  
Barcelona Research Center for Multiscale Science and Engineering  
Universitat Politècnica de Catalunya  
C/ Eduard Maristany, 10-14, 08019, Barcelona, Spain  
E-mail: [jordi.puiggali@upc.edu](mailto:jordi.puiggali@upc.edu) and [carlos.aleman@upc.edu](mailto:carlos.aleman@upc.edu)

[c] Dr. G. Ballano and Prof. Dr. C. Cativiela  
Department of Organic Chemistry and Instituto de Síntesis Química y Catalisis Homogenea (ISQCH)  
University of Zaragoza-CSIC  
50009 Zaragoza, Spain  
E-mail: [cativiela@unizar.es](mailto:cativiela@unizar.es)

[d] Dr. M. Font-Bardia  
Departament de Mineralogia, Cristallografia i Depòsits Minerals  
Universitat de Barcelona  
Facultat de Geologia, c/Martí i Franquès, E-08028, Spain

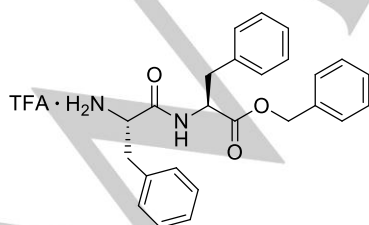
[e] Dr. M. Font-Bardia  
Unitat de Difracció de Raigs X, Centre Científic y Tecnològic  
Universitat de Barcelona  
C/Solé i Sabarís 1, Barcelona E-08028, Spain

Supporting information for this article is given via a link at the end of the document

Another investigated strategy was the co-assembly of FF-based biomaterials with other molecules bearing aromatic groups.<sup>[21–24]</sup> This approach, which may provide intermolecular transfer mechanisms,<sup>[25,26]</sup> was applied to the Npm-FF (Npm = naphthoxymethyl) donor / dansyl acceptor system.<sup>[21]</sup> Peptide fibres based partly on aromatic stacking interactions with the dansyl component intercalated within this structure exhibited a redshift in the fluorescence emission and the corresponding quenching of the emission associated with the donor species.<sup>[21]</sup> Besides, hydrogels derived from the co-assembly of Fmoc-FF and Fmoc-diglycine<sup>[22]</sup> (Fmoc-GG) or Fmoc-Arg-Gly-Asp (Fmoc-RGD)<sup>[23]</sup> showed higher elastic moduli than Fmoc-FF alone, while the combination of Fmoc-FF with Fmoc-Lys (Fmoc-K), Fmoc-Ser (Fmoc-S) or Fmoc-Asp (Fmoc-D) resulted in significant changes in the rheological properties and fiber morphology.<sup>[24]</sup>

Besides, solvent-induced structural transitions have been examined by different authors. Li and co-workers<sup>[27]</sup> reported the transition of an organogel obtained by self-assembly of FF in toluene into a lower-like microcrystal merely by introduced ethanol as co-solvent. Huang *et al.*<sup>[28]</sup> reported the structural transition of self-assembled FF from microtubes to nanofibers by introducing acetonitrile as co-solvent in water phase. Mumaraswamy *et al.*<sup>[29]</sup> found that the dimensions of FF nanotubes are strongly influenced not only by the temperature and pH but by the ionic strength of the solution. Mba and co-workers<sup>[30]</sup> synthesized two organogelators based on a pyrene moiety linked to FF, which formed spherical aggregates and entangled fibrillary networks in acetonitrile and *o*-dichlorobenzene, respectively. Wang *et al.*<sup>[31]</sup> used FF to prove that a trace amount of solvents can be a predominant factor to tune peptides self-assembly. More specifically, these authors showed that the addition very small amounts of solvents can be used to force solvent-bridged hydrogen bonds, which is a crucial interaction in directing fiber formation.

In this paper we use the solvent mixing method (*i.e.* dissolving the peptide in OS and adding water or another OS as co-solvent) to examine the self-assembly of a new FF-based amphiphile. In this new compound, hereafter denoted TFA·FF-OBzl (Scheme 1), the C-terminus is capped with a benzyl ester (OBzl) group and the protonated amino group is stabilized forming an ion pair with trifluoroacetate (TFA). Accordingly, aromatic interactions are expected to be weaker than on Fmoc-FF, Nap-FF and Fmoc-FF-OFm, while the dominant role played by intermolecular electrostatic interactions in FF is expected to decrease considerably because of the stability provided by the TFA.



**Scheme 1.** Chemical structure of TFA·FF-OBzl

## Results and Discussion

Results presented in this work correspond to the conditions in which repetitive, stable and structured morphologies were observed. More specifically, assemblies have been required to fulfill the following conditions: i) to present a clearly defined morphology; ii) to be systematically observed when the same conditions are used in different and independent experiments; and iii) to remain formed upon manipulation for optical microscopy, SEM and/or AFM observations).

### Peptide synthesis and Preparation of initial TFA·FF-OBzl solutions

The synthesis of TFA·FF-OBzl was carried out following the procedure provided in Figure 1.

As the main aim of this study is to investigate the influence of both the polarity of the medium and the peptide concentration in the assembly of TFA·FF-OBzl a two-step procedure was used. Firstly, concentrated (5.0 mg/mL) stock solutions were prepared using solvent able to completely dissolve the peptide. For this purpose, four solvents with very different polarities were selected: hexafluoroisopropanol (HFIP), dimethylformamide (DMF), DMSO and milli-Q water. The dielectric constants of such solvents are:  $\epsilon = 16.7$  (HFIP), 37.2 (DMF), 46.7 (DMSO) and 78.5 (water). Secondly, the peptide concentration and the polarity of the medium were altered by direct addition of a co-solvent to the stock solution. In addition, of the above mentioned solvents, both methanol (MeOH,  $\epsilon = 32.6$ ), chloroform (CHCl<sub>3</sub>,  $\epsilon = 4.7$ ), which are not able to completely dissolve the peptide, were considered as co-solvent. This procedure allowed varying the peptide concentration in the prepared solvent : co-solvent mixtures between 0.05 to 4.8 mg/mL. Both the final peptide concentration and the chemical nature of the mixture will be provided for each discussed structure.

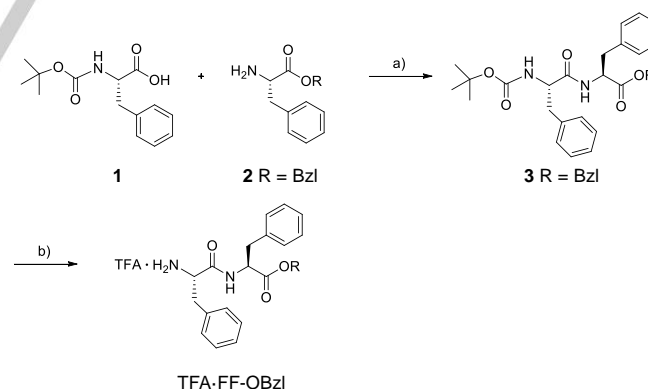


**Figure 1.** Scheme of the reactions used to obtain TFA·FF-OBzl. Reagents and conditions: (a) EDC, HOBT, DIPEA CH<sub>2</sub>Cl<sub>2</sub>, 0°C 30 min, room temperature 24 h; (b) TFA, CH<sub>2</sub>Cl<sub>2</sub>, room temperature 1 h.

For the formation of the assembled structures, 10 or 20  $\mu$ L aliquots of the prepared peptide solutions were placed on microscope coverslips or glass slides (glass sample holders) and kept at room temperature (21 °C) or inside a cold chamber

(4 °C) until dryness. The humidity was kept constant in both laboratories at 50%. It is worth noting that no thermal treatment was applied to improve the solubility of the peptide or to accelerate the evaporation of the solvents. In spite of the huge number of conditions examined, the structures obtained from all them were carefully examined by optical microscopy. However, only those structures that fulfill the requirements described above (*i.e.* well-defined morphology and reproducibility) were subsequently studied by SEM and AFM for discussion in this work.

### Aqueous environment

Dissolution of TFA-FF-OBzl into 2.0 mg/mL 4:6 HFIP:water directed the self-assembly process towards peptide nanofibers with a diameter ( $\phi$ ) of  $\sim$ 250 nm that align and pack forming well-defined microfibers of up to  $\sim$ 10  $\mu$ m (Figure 2a). At the same time, such microfibers form very dense aggregates with a spike-like morphology. When the polarity of the mixture increases and the peptide concentration decreases in 0.1 mg/mL 1:49 HFIP:water, the density of aggregated microfibers decreases, whereas a very porous mesh of randomly oriented (bundled) fibers coexists coating partially the spike-like supramolecular structure (Figure 2b). These bundled fibers exhibit very different diameters (*i.e.* from  $\sim$ 100 nm to  $\sim$ 1  $\mu$ m) and do not present any kind of imperfection, as it can be observed in the corresponding SEM and AFM images. The mesh is replaced by small needle-like crystals emerging from the spike-like microstructures in 1.0 mg/mL 1:4 DMF:water peptide solutions (Figure 2c). However, a remarkable difference is that such spikes are not formed by long aligned nanofibers, as observed in Figure 2a for the 2.0 mg/mL 4:6 HFIP:water mixture, but by relatively short and sometimes broken interconnected nanofibers. These results suggest that the structure of the nanofibers, as well as their supramolecular organization (*i.e.* the hierarchical self-assembly of TFA-FF-OBzl), change with both the polarity of the solvent mixture and the concentration of the peptide.

The addition of diluted KCl aqueous solutions (50 mM) to the HFIP, DMF or DMSO peptide solutions caused drastic morphological changes, which mainly consists in the apparition of branched-like structures and, in some cases, ultra-thin plates. Thus, poorly defined micrometric branched-like architectures (Figure 3a), which coexist with peptide microfibers (Figure S1a), grow from 4.8 mg/mL 24:1 HFIP:50mM-KCl(aq) peptide solutions. However, microfibers coated with salt and abundant defects (Figure S1b) are the only structures observed upon reduce the peptide concentration to 1.0 mg/mL. Besides, branched-like structures (Figure 3b), coexisting with disordered microfibers agglomerates (Figure S2), are obtained in 1.0 mg/mL 1:4 DMF:50mM-KCl(aq). The branching is much better defined than in Figure 3a, suggesting that this class of architecture is promoted by enhancing both the polarity of the mixture and the ionic force.

The large influence of the polarity is corroborated in Figure 3c for the 4.8 mg/mL 24:1 DMSO:50mM-KCl(aq) peptide mixture. In this case very-well defined branched structures, each one nucleating from a spherulite, and partially coated with cubic crystals of salt are abundantly detected. Both the central

spherulite and the branches are made of ultra-thin plates that, despite resembling lamellar crystal structures, are obtained through the hierarchical assembly of nanowires. When the peptide concentration decreases to 2.0 mg/mL and, consequently, the polarity and ionic strength of the 4:6 DMSO:50mM-KCl(aq) mixture increase, branches become worsen defined and less abundant (Figure S3), even though self-assembly characteristics are similar to those described above for the concentrated peptide solution. Moreover, these supramolecular structures coexist with randomly distributed micrometric crystals of oval shape (Figure 3d). Finally, when the peptide concentration is reduced, as for example in 0.25 mg/mL 1:19 DMSO:50mM-KCl(aq), spherulitic-like microstructures surrounded by large salt crystals are observed (Figure 3e). According to the micrographs displayed in Figure 3c-e and S3, the combination of a polar OS (*i.e.*  $\epsilon = 46.2$  for DMSO) with an aqueous salt solution, KCl(aq), results in a hierarchical assembly of the amphiphilic peptide under study, even though this tendency becomes less pronounced with decreasing amount of DMSO (*i.e.* higher ionic strength). This feature should be associated to the influence of solvent molecules and salt ions on the balance between peptide-peptide and peptide-solvent interactions.

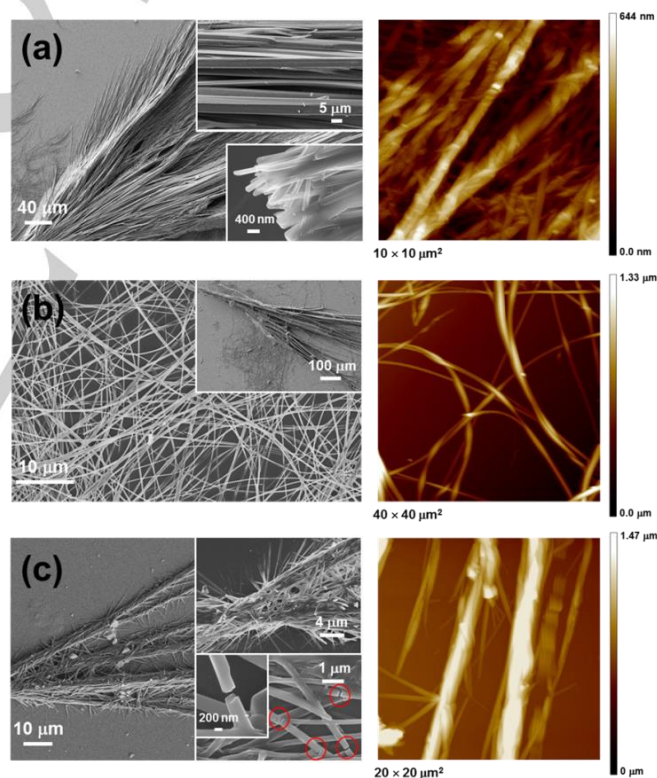


**Figure 2.** Representative SEM and AFM (height) images of the structures derived from TFA-FF-OBzl solutions in: (a) 2.0 mg/mL 4:6 HFIP:water at 4 °C; (b) 0.1 mg/mL 1:4 HFIP:water at room temperature; and (c) 1.0 mg/mL 1:4 DMF:water at room temperature. The shape and hierarchical self-assembly changes with polarity of the solvents mixture and the peptide concentration. Red circles in (c) indicate broken nanofibers.

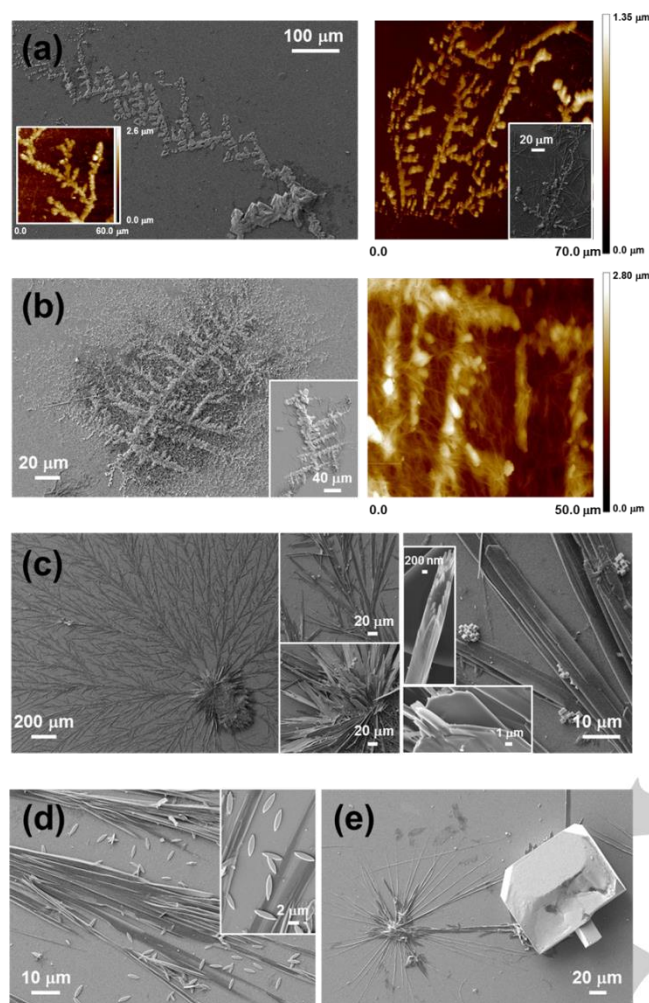


**Figure 3.** Representative SEM and AFM (height) images of the branched structures obtained at room temperature from TFA·FF·OBzl dissolved in: (a) 4.8 mg/mL 24:1 HFIP:50mM-KCl(aq); (b) 1.0 mg/mL 1:4 DMF:50mM-KCl(aq); (c) 4.8 mg/mL 24:1 DMSO:50mM-KCl(aq); (d) 2.0 mg/mL 4:6 DMSO:50mM-KCl(aq); and (e) 0.25 mg/mL 1:19 DMSO:50mM-KCl(aq).

The formation of branched-like structures is also considerably affected by the pH. This is reflected in Figure S4, in which the pH of the corresponding OS : 50mM-KCl(aq) solutions was fixed at 10.5 by adding 0.5 M NaOH. The poorly defined branched structures mentioned above for the 4.8 mg/mL 24:1 HFIP:50mM-KCl(aq) mixture (Figure 2a) results into very well defined tree-like structures of fibrous nature at basic pH (Figure S4a). In contrast, the addition of NaOH transforms the spherulite-nucleated branches observed in Figure 2c into dense bundles of plates irregularly arranged (Figure S4b). Indeed, some of these plates resemble deformed microtubes because of their dimensions. This is reflected by the AFM cross sectional profile displayed in Figure S4b, which shows that the x- and y-diameter for one of such elements is  $\sim 2.3$  and  $\sim 2.0$   $\mu\text{m}$ , respectively. These changes have been attributed to the neutralization of the peptide by the NaOH. Thus, strong and non-specific (non-

directional) electrostatic interactions associated to the charged end groups are probably replaced by weak and specific (directional) hydrogen bonds after neutralization, affecting the definition of the assemblies their growing.

It should be remarked that the branched- and tree-like structures obtained for TFA·FF·OBzl do not resemble the dendritic structures identified for FF<sup>[32]</sup> and Fmoc-FFFF-Fmoc.<sup>[20]</sup> Kim and co-workers<sup>[32]</sup> obtained highly ordered multi-dimensional dendritic nanoarchitectures by self-assembling FF from an acidic buffer solution. More recently, stable dendritic structures made of branches growing from nucleated primary frameworks were observed for Fmoc-FFFF-OFm.<sup>[20]</sup> The fractal dimension of FF and Fmoc-FFFF-OFm dendrimers was determined to be 1.7, which evidenced self-similarity and two-dimensional diffusion controlled growth.<sup>[20,32]</sup> However, branched and tree-like structures displayed in Figures 3 and S4a do not exhibit a primary nucleating framework nor a repetitive pattern for growing of the branches, which are essential to obtain the characteristic self-similarity of dendritic structures.

#### Single crystal X-ray structure of TFA·FF·OBzl

X-ray diffractograms were collected for prism-like crystals obtained by slow evaporation at 80 °C of a 0.415 mg/mL solution of TFA·FF·OBzl in milliQ- water. Table S1 summarizes the main crystallographic data of TFA·FF·OBzl, whereas Table S2 shows the final atomic parameters (fractional coordinates and thermal factors) together with the estimated standard deviations. Geometric parameters are listed in Tables S3 (bond lengths and angles) and Table S4 (torsional angles).

Conformation of a single TFA·FF·OBzl molecule is shown in Figure 4a together with labelling of atoms and the corresponding displacement ellipsoids. It is clear that the molecule adopted a folded conformation, being the peptide group practically planar (C10-N1-C1-C2 of  $-173.3^\circ$ ) and the  $\varphi$  (C1-N1-C10-C11) and  $\psi$  (N2-C2-C1-N1 / N1-C10-C11-O3) torsional angles of  $-86.6^\circ$  and  $127.7^\circ / -54.9^\circ$ , respectively. It is worth noting that such conformation does not fit to that expected for a conventional  $\beta$ -strand within a  $\beta$ -sheet, which typically exhibits  $\varphi, \psi$  values around  $-135^\circ, +135^\circ$ . This feature has been attributed to the formation of an intramolecular  $\pi$ - $\pi$  stacking interaction between the C13-C18 benzyl (Bzl) and C20-C25 phenyl (Ph) rings, which is indicated by a red arrow in Figure 4a. The dihedral angle between the Bzl and Ph aromatic groups is  $33.6^\circ$ , while the distance between the centroids of the two rings is 4.59 Å.

TFA·FF·OBzl crystallizes in an orthorhombic unit cell containing 4 molecules (Figure S5) which are related by binary screw axes as typical of chiral organic molecules. Figure 4b depicts a scheme of the molecular packing (*b-c* projection) with two neighboring molecules. The existence of a hydrophilic core, which is formed by the carboxylate (from TFA), ester and amide groups, is particularly noticeable. This hydrophilic core is surrounded by a hydrophobic crown (dashed circle) formed by ten aromatic rings (*i.e.* 6 phenyl and 4 benzyl rings). Only six of these rings belong to the two represented molecules whereas the other four are associated to neighboring ones. Table S5 summarizes the hydrogen bond interactions that can be considered and that involve ester, amide and carboxylate groups.

The most relevant intermolecular hydrogen bond, which is formed along the *a* direction, involves the N–H (amide) and C=O (ester) groups of molecules with a parallel orientation as displayed in Figure 4c. It is remarkable that the C=O of amide groups only forms a weak interaction with terminal NH<sub>3</sub><sup>+</sup> groups. Finally, an intermolecular  $\pi$ – $\pi$  stacking interactions involving C4–C9 (Ph)···C13–C18 (Bzl) and C4–C9 (Ph)···C20–C25 (Ph) aromatic rings are also present, being the distance between the centroids around 4.5 Å.

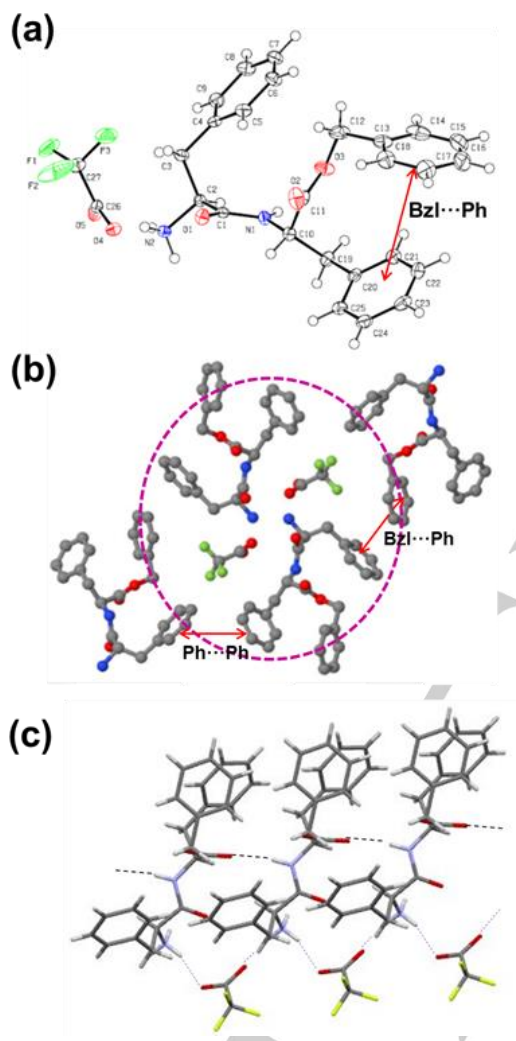


**Figure 4.** (a) Scheme of the TFA-FF-OBzl molecule with displacement ellipsoids drawn at the 50% probability level. H atoms are drawn as circles with arbitrary radii. (b) View along the *c* axis showing the packing of two molecules related by a binary screw axis. Dashed circle points out the aromatic rings that are disposed around the inner hydrophilic part. H atoms have been omitted for clarity. (c) Scheme showing the intermolecular hydrogen bonds established between neighboring chains along the *a* axis.

Peptide···peptide intermolecular electrostatic, hydrogen bonds and  $\pi$ – $\pi$  stacking interactions are known to be an essential contributor to the formation of FF nano- and microarchitectures.<sup>[33]</sup> According to its crystal structure, the importance of these intermolecular forces is maintained in

assembly of the TFA-FF-OBzl amphiphile. Thus, based on the morphology of the morphology of the assembled structures and in the position of the molecules in the crystal structure reported in this work, as the solvent gradually evaporates, the individual TFA-FF-OBzl tend to form intermolecular electrostatic and  $\pi$ – $\pi$  stacking interactions, promoting the aggregation of the peptide molecules and the formation of amphiphile crowns. The formation of hydrophobic crown in the aggregates is reinforced by the intramolecular  $\pi$ – $\pi$  stacking interactions. These interactions results in the formation of  $\beta$ -sheet structures, which stack vertically via hydrogen bonds resulting in the lengthening of the peptide structures. This process is similar to that reported for the amyloid fibril formation, even though and that case aggregates are usually formed through electrostatic and hydrogen bonding interactions (*i.e.*  $\pi$ – $\pi$  stacking interactions frequently participates in the lengthening of the structures).<sup>[34]</sup>

### Organic environment

Dissolution of the peptide in a single OS resulted in turbid solutions with white particles (flocs) in suspension, the combination of two OSs being necessary to obtain clear solutions and the subsequent self-assembly processes. Different levels of organization were obtained depending on both the polarity of the mixture. Results are summarized in Figure 5.

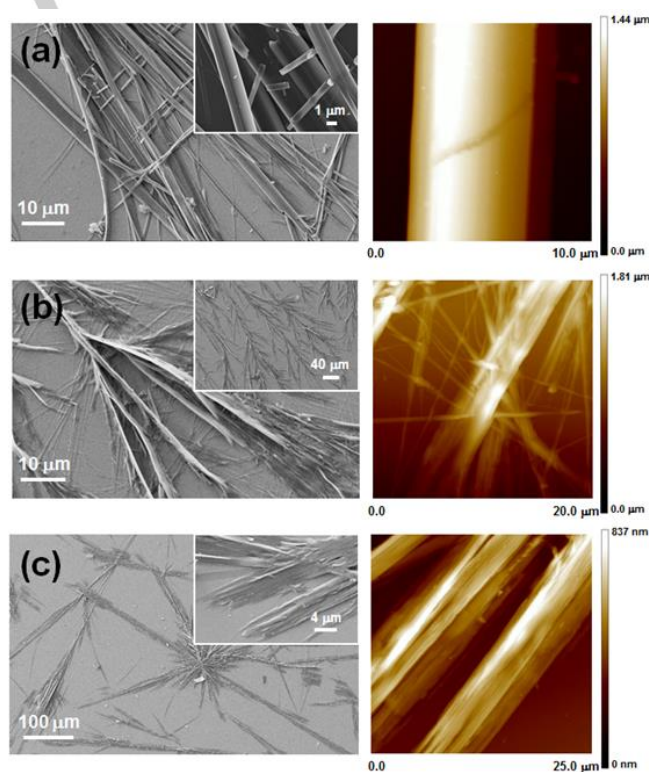


**Figure 5.** Representative SEM and AFM (height) images of the structures obtained at room temperature from TFA-FF-OBzl dissolved in: a) 4.0 mg/mL DMF:MeOH; (b) 4.0 mg/mL HFIP:MeOH; and (c) 4.0 mg/mL HFIP:CHCl<sub>3</sub>. Fiber-like organizations evolve towards plate-like organizations with decreasing polarity of the medium. The dielectric constant of DMF, HFIP, MeOH and CHCl<sub>3</sub> is  $\epsilon = 37.2, 16.7, 32.6$  and  $4.7$ , respectively.

Concentrated peptide solutions ( $\geq 4$  mg/mL) in polar organic mixtures, as DMF:MeOH, result in well-defined microfibers ( $\phi$  ranging from 2.5 to 5.5  $\mu\text{m}$ ) with a smooth surface (Figure 5a), which tend to adopt a preferential alignment, crossed perpendicularly by fibers of smaller diameter ( $\phi \approx 0.7\text{--}0.9$   $\mu\text{m}$ ). Microfibers transform into microplates when the polarity of the environment decreases ( $\geq 4$  mg/mL HFIP:MeOH), whereas crossed submicro-fibers change the perpendicular orientation by a tilted one ( $\sim 45^\circ$ ). Thus, the most remarkable feature caused by the reduction of the polarity is the branched-like supramolecular organization of the peptide (Figure 5b). This feature becomes more pronounced in the least polar environment (4.0 mg/mL HFIP:CHCl<sub>3</sub>), where spherulitic-like structures made of microplates are frequently identified (Figure 5c).

It should be mentioned that structures obtained using low peptide concentrations were disordered (*i.e.* without well-defined morphology) and poorly reproducible in all cases. As an hypothesis, this has been attributed to the fact that the organization of the amphiphilic molecules forming hydrophobic crowns is difficult in organic solvents, which evaporate faster than water. Thus, a high amount of peptide molecules are presumably required to form regular structures with well-defined morphologies, like those displayed in Figure 5.

Overall, results in OSs indicate that the polarity of the environment regulates the 3D arrangement of the sheets formed by TFA-FF-OBzl molecules, controlling the formation of tubes or plates. On the other hand, comparison of supramolecular organizations observed in aqueous and OSs reflect two general trends that are characteristics of the latter environment. Firstly, the concentration of peptide required to obtain well-defined self-assembly processes in organic environments is significantly higher ( $\geq 4$  mg/mL) than in aqueous solvents. Thus, in organic environments peptide-solvent interactions are energetically favored with respect to peptide-peptide interactions. This suggests that, in water-containing solutions (*i.e.* those with higher polarity), attractive interactions between polar groups and water are far from compensating the repulsive interactions between such solvent and the aromatic groups of the peptide. Secondly, the density of supramolecular structures is considerably higher in water-containing environments than in OSs, which corroborates our previous hypothesis. Thus, the interaction of the peptide with the organic solvent is less repulsive than with water, hindering the self-assembly process in the former environment.

#### Influence of the surrounding environment in the assembly mechanism

The single crystal structure of TFA-FF-Bzl, which was obtained by slow evaporation from a pure water solution, evidenced the construction of a network of hydrogen bonds formed by parallel strands, which also interact through intra- and inter-molecular stacking interactions (Figure 4). Although the parallel disposition of the molecules is in agreement with that observed by Adams and co-workers for single crystals of Fmoc-FF collected from gels formed in acetone,<sup>[18]</sup> important differences are detected between such two structures. These correspond to the drastic separation between hydrophilic and hydrophobic groups in

TFA-FF-OBzl. Thus, the latter exhibits a hydrophobic crown surrounding a hydrophilic core that contains all the polar groups, whereas such separation is much less pronounced in Fmoc-FF because of the steric hindrance induced by the bulky Fmoc groups.<sup>[18]</sup> The clear separation between polar groups and hydrophobic rings in TFA-FF-OBzl facilitates the understanding of the influence of the solvent on the morphology of self-assembled aggregates. Thus, the crystal structure of TFA-FF-OBzl has been considered as representative for understanding the behavior of amphiphilic FF-based biomaterials in different environments.

Peptide nano- and microfibers obtained in OS:water environments with low and very low peptide concentrations (*i.e.* mixtures in which the high dielectric constant of water plays a dominant role because of its high volume ratio with respect to the OS) has been attributed to an assembly in which hydrophobic and polar forces are equally important to promote the longitudinal growing of the fiber, whereas the interactions between the fiber surface and both the environment and the glass support are stabilized by polar forces. Accordingly, the length of the fiber increases because of the favorable hydrophobic-hydrophobic and polar-polar interactions between regions of identical nature, while polar groups remain exposed at the surface of the fibers (Figure 6a). Moreover, this simple model explains that, for a given OS, the density of aggregated fibers decreases when the volume ratio of water as co-solvent increases (*i.e.* the polarity of the mixture increases). Thus, the favorable interactions between the peptide polar groups and water molecules compensate the affinity between the surface polar groups of different fibers when the concentration of water in the solvents mixture is high enough.

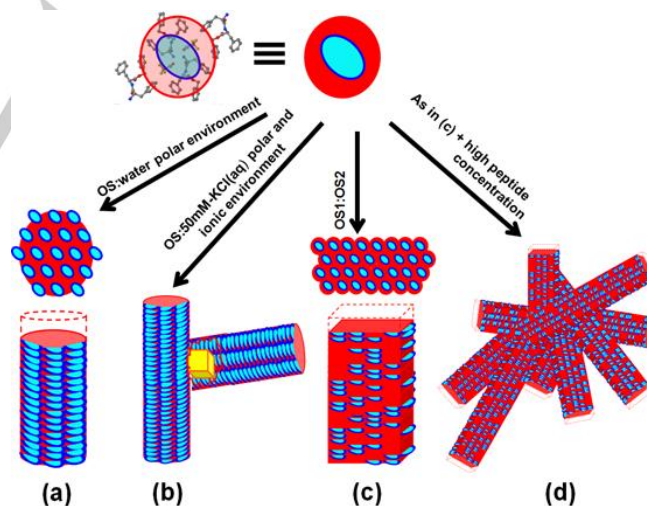


**Figure 6.** Schemes explaining the self-assembly and aggregation of TFA-FF-OBzl in different conditions considering the hydrophilic (blue) and hydrophobic (red) regions observed in the corresponding X-ray structure (Figure 4): (a) fibers; (b) branched fibers; (c) plates; and (d) spherulites.

The enhancement of the ionic strength in OS:water peptide solutions, which is achieved by replacing the milli-Q water by a 50 mM KCl aqueous solutions as added co-solvent, results in

the formation of microstructures with branched-like architectures coexisting with continuous (non-branched) fibers. Both the observation of cubic KCl crystals and the reduction of continuous fibers with increasing ionic strength are consistent with the mechanism like that displayed in Figure 6b. According to this, the formation of salt nanocrystals coating the surface of peptide fibers nucleates the branches that grow through favorable  $\text{KCl}\cdots\text{TFA}\cdot\text{FF}\cdot\text{OBzl}$  electrostatic interactions. The frequency of this branching process increases with the ionic strength of the mixture, which explains the fact that the definition of the branched-like architectures and the presence of non-branched fibers decrease with increasing volume ratio of KCl aqueous solution in the OS:co-solvent mixture.

Microstructures derived from the combination of two OSs also depend on the polarity of the mixture. Polar environments with high peptide concentrations result in the formation of microfibrils by a mechanism similar to that displayed in Figure 6a, transforming into microplates when the polarity of the environment decreases. In order to reduce the access of the hydrophilic core to the surface, a mechanism like that depicted in Figure 6c is proposed. In this mechanism, the 2D growing of the microstructure and the predominant hydrophobic region at the boundary favor the formation of peptide-solvent interactions. Moreover, as the polarity of the environment is not drastically low, the apparition of irregularities and defects with the hydrophilic core exposed to the solvent does not represent a severe thermodynamic penalty for the microstructure generation. At high peptide concentrations, the affinity between the hydrophobic surface regions provokes the aggregation of plates, as is displayed in Figure 6d, giving place to spherulites.

Overall, results displayed in this work combined with the straightforward models schematized in Figure 6 provide a simple rational that explains the assembly behavior of the  $\text{TFA}\cdot\text{FF}\cdot\text{OBzl}$  amphiphile. Accordingly, the morphology of microstructures derived from this peptide can be easily regulated by controlling both the solvent and the peptide concentration. This versatility makes  $\text{TFA}\cdot\text{FF}\cdot\text{OBzl}$  a very interesting system for applications that are mainly based on interactions with other chemical species, as for example drugs. Within this context,  $\text{TFA}\cdot\text{FF}\cdot\text{OBzl}$  microstructures are potential candidates to upload either polar or non-polar drugs at their surface and, therefore, be used as versatile carriers and/or delivery systems. Thus, although some peptide amphiphiles have been previously suggested for delivery,<sup>[35,36]</sup> their utility is typically restricted to the loading of polar or non-polar drugs. However, the adaptability of  $\text{TFA}\cdot\text{FF}\cdot\text{OBzl}$  eliminates the restrictions related with the chemical nature of the used drugs, giving a new dimension to this application.

## Conclusions

We have evidenced the remarkable control exerted by the characteristics of the solvents mixture on the organization of  $\text{TFA}\cdot\text{FF}\cdot\text{OBzl}$  assemblies derived from the addition of a co-solvent to peptide solution. Thus, the polarity, ionic strength and peptide concentration in the mixture have been regulated by adding a selected amount of a given co-solvent (*i.e.* pure water,

50mM-KCl(aq) or an OS) to a concentrated peptide solution in HFIP, DMF, DMSO or water. Although polar aqueous environments tend to promote the growth of fibers, which coexist with branched-like microstructures when milli-Q water is replaced by 50mM-KCl(aq), non-polar environments obtained by mixing two OSs prefer peptide assemblies organized in plates and spherulites.

X-ray diffractograms collected for  $\text{TFA}\cdot\text{FF}\cdot\text{OBzl}$  single crystals reveal a segregated distribution of hydrophilic and hydrophobic regions. More specifically, the carboxylate (from TFA), amide and ester (both from  $\text{FF}\cdot\text{OBzl}$ ) groups from a highly polar core stabilized through hydrogen bonding interactions, which is ringed by a hydrophobic crown involving 10 aromatic rings. This unique organization has enabled us to explain the influence of the solvents mixture properties on the peptide assembly. Thus, the growing of the peptide structure and the exposition of hydrophilic or hydrophobic regions is simply determined by the formation of favorable peptide-solvent interactions at the surface. Tuning the structure of  $\text{TFA}\cdot\text{FF}\cdot\text{OBzl}$  by changing the solvents used in the mixture is a very attractive feature to expand the potential utility of peptide assemblies in different fields, for example as molecular carriers and delivery systems. Thus, both polar and non-polar compounds could be easily loaded on  $\text{TFA}\cdot\text{FF}\cdot\text{OBzl}$  microstructures by regulating the assembly through the solvents used in mixture.

## Experimental Section

**Peptide synthesis and characterization.** Melting points were determined on a Gallenkamp apparatus and are uncorrected. IR spectra were registered on a Nicolet Avatar 360 FTIR spectrophotometer;  $\nu_{\text{max}}$  is given for the main absorption bands.  $^1\text{H}$  and  $^{13}\text{C}$  NMR spectra were recorded on a Bruker AV-400 or ARX-300 instrument at room temperature, using the residual solvent signal as the internal standard. Chemical shifts ( $\delta$ ) are expressed in ppm and coupling constants ( $J$ ) in Hertz. Optical rotations were measured on a JASCO P-1020 polarimeter. High-resolution mass spectra were obtained on a Bruker Microtof-Q spectrometer.

**Boc-FF-OBzl (3).** To a solution of Boc-F-OH (**1**) (1.75 g, 6.6 mmol) in dichloromethane (15 mL) cooled to 0 °C in an ice bath, was added 1-hydroxybenzotriazole hydrate (HOBt) (1.01 g, 6.6 mmol) followed by *N*-[3-(dimethylamino)-propyl]-*N'*-ethylcarbodiimide hydrochloride (EDC-HCl) (1.27 g, 6.6 mmol) and the reaction was stirred for 15 min. Then, a solution of the amino component H-F-OR (**2**) (6.0 mmol) [obtained by addition of *N,N*-diisopropylethylamine (DIPEA) (1.25 mL, 7.2 mmol) to the TFA salt of **2**] in dichloromethane (5 mL) and additional *N,N*-diisopropylethylamine DIPEA (1.15 mL, 6.6 mmol) were added. The reaction was stirred for 1 h at 0 °C, then at room temperature for 24 h. The reaction mixture was washed with 5% aqueous solution of  $\text{NaHCO}_3$  ( $3 \times 15$  mL), followed by 5% aqueous solution of  $\text{KHSO}_4$  ( $3 \times 15$  mL). The organic phase was dried over anhydrous magnesium sulfate and evaporated to dryness. The resulting solid was suspended in a diethyl ether/*n*-hexane mixture and filtered at reduced pressure to provide **3** as a white solid.

Yield: 90%. Mp: 180–181 °C.  $[\alpha]_{\text{D}}^{25}$ : -17.7 ( $c = 0.33$ , methanol). IR (KBr)  $\nu$ : 3332, 1741, 1696, 1681  $\text{cm}^{-1}$ .  $^1\text{H}$  NMR ( $\text{CDCl}_3$ , 400 MHz):  $\delta$  1.32 (s, 9H), 2.92–3.02 (m, 4H), 4.21–4.30 (m, 1H), 4.72–4.76 (m, 1H), 4.86 (bs, 1H),

5.02 (s, 2H), 6.20 (d, 1H,  $J = 7.6$  Hz), 6.81–6.83 (m 2H), 7.07–7.14 (m, 5H), 7.16–7.21 (m, 5H), 7.26–7.32 (m, 3H).  $^{13}\text{C}$  NMR ( $\text{CDCl}_3$ , 100 MHz):  $\delta$  28.36, 38.07, 38.43, 53.44, 55.82, 67.35, 80.32, 127.11, 127.19, 128.65, 128.67, 128.70, 128.74, 128.79, 129.41, 129.49, 135.14, 135.61, 136.62, 155.39, 170.85, 170.90. HRMS (ESI)  $\text{C}_{30}\text{H}_{34}\text{N}_2\text{NaO}_5$   $[\text{M}+\text{Na}]^+$ : calcd. 525.2360, found 525.2375.

For Boc deprotection, a solution of the corresponding Boc-protected compound in dichloromethane was treated with trifluoroacetic acid (TFA; 15 equiv.) and the reaction mixture was stirred at room temperature for 1 h. After evaporation of the solvent, the residue was suspended in a diethyl ether/*n*-hexane mixture and filtered at reduced pressure to provide the corresponding TFA salt as a white solid in quantitative yield.

**TFA-FF-OBzl (4).** According to the general Boc deprotection procedure, TFA (2 mL) was added to a solution of **3** (2.0 mmol) in dichloromethane (20 mL) to provide the corresponding TFA salt **4** (Figure S6) in quantitative yield.

Mp: 290–292 °C dec.  $[\alpha]_{\text{D}}^{20}$ : 18.2 ( $c = 0.36$ , acetic acid). IR (KBr)  $\nu$ : 3342, 1725, 1695, 1662  $\text{cm}^{-1}$ .  $^1\text{H}$  NMR (DMSO, 400 MHz):  $\delta$  2.90 (dd, 1H,  $J = 14.2$  Hz,  $J = 8.3$  Hz), 3.02 (dd, 1H,  $J = 13.9$  Hz,  $J = 8.1$  Hz), 3.08–3.13 (m, 2H), 4.05–4.13 (m, 1H), 4.63–4.69 (m, 1H), 5.06–5.14 (m, 2H), 7.22–7.38 (m, 15H), 8.23 (bs, 2H), 9.15 (d, 1H,  $J = 7.5$  Hz).  $^{13}\text{C}$  NMR (DMSO, 100 MHz):  $\delta$  36.79, 36.99, 53.21, 54.03, 66.37, 111.85, 114.77, 117.68, 120.60, 126.80, 127.19, 128.09, 128.20, 128.45, 128.54, 129.18, 129.59, 134.79, 135.60, 136.65, 158.05, 158.40, 158.75, 159.10, 168.43, 170.71. HRMS (ESI)  $\text{C}_{25}\text{H}_{26}\text{N}_2\text{NaO}_3$   $[\text{M}+\text{Na}]^+$ : calcd. 425.1836, found 425.1821.

**Samples preparation.** Peptide containing solutions (25 or 100  $\mu\text{L}$ ) were prepared from 5 mg/mL stocks using HFIP, DMF, DMSO or milli-Q water as solvents. The peptide concentration was reduced by adding milli-Q water, MeOH or  $\text{CHCl}_3$ , as co-solvent, to a given stock solution. More specifically, peptide concentrations of 4.8, 4.0, 2.0, 1.0, 0.3, 0.25 and 0.1 mg/mL were obtained using 24:1, 4:1, 4:6, 1:4, 3:47, 1:19 and 1:49 solvent:co-solvent ratios, respectively. On the other hand, the 50mM-KCl(aq) solution was used as co-solvent to modify the ionic strength. Finally, 10 or 20  $\mu\text{L}$  aliquots were placed on microscope coverslips and kept at room temperature (25 °C) or inside a cold chamber (4 °C) until dryness. All organic solvents were purchased from Sigma-Aldrich, Fisher Scientific and Scharlab.

**Optical microscopy.** Morphological observations were performed using a Zeiss Axioskop 40 microscope. Micrographs were taken with a Zeiss AxiosCam MRC5 digital camera.

**Scanning electron microscopy (SEM).** SEM studies were performed in a Focussed Ion Beam Zeiss Neon 40 scanning electron microscope operating at 5 kV and equipped with an EDX spectroscopy system. Samples were mounted on a double-side adhesive carbon disc and sputter-coated with a thin layer of carbon to prevent sample charging problems.

**Atomic Force Microscopy (AFM).** Topographic AFM images were obtained using either a Dimension 3100 Nanoman AFM or a Multimode, both from Veeco (NanoScope IV controller) under ambient conditions in tapping mode. AFM measurements were performed on various parts of the morphologies, which produced reproducible images similar to those displayed in this work. Scan window sizes ranged from  $5 \times 5 \mu\text{m}^2$  to  $80 \times 80 \mu\text{m}^2$ .

**Crystallization and X-ray diffraction.** Colorless prism-like crystals ( $0.010 \text{ mm} \times 0.020 \text{ mm} \times 0.100 \text{ mm}$ ) were obtained by slow evaporation

at 80 °C of a 0.415 mg/mL solution of TFA-FF-OBzl in MQ-grade water and used for X-ray diffraction analysis. The X-ray intensity data were measured on a D8 Venture system equipped with a multilayer monochromator and a Cu microfocus ( $\lambda = 1.54178 \text{ \AA}$ ).

The frames were integrated with the Bruker SAINT software package using a narrow-frame algorithm. The integration of the data using an orthorhombic unit cell yielded a total of 13671 reflections to a maximum  $\theta$  angle of 79.25° (0.78  $\text{\AA}$  resolution), of which 5037 were independent (average redundancy 2.714, completeness = 95.0%,  $R_{\text{int}} = 4.97\%$ ,  $R_{\text{sig}} = 5.67\%$ ) and 4499 (89.32%) were greater than  $2\sigma(F^2)$ . The final cell constants of  $a = 5.8856(3) \text{ \AA}$ ,  $b = 18.5677(9) \text{ \AA}$ ,  $c = 23.0370(11) \text{ \AA}$ , volume =  $2517.5(2) \text{ \AA}^3$ , are based upon the refinement of the XYZ-centroids of reflections above  $2\theta$  ( $\sigma(I)$ ). Data were corrected for absorption effects using the multi-scan method (SADABS). The calculated minimum and maximum transmission coefficients (based on crystal size) are 0.6156 and 0.7461.

The structure was solved and refined using the Bruker SHELXTL Software Package, using the space group  $P2_12_12_1$ , with  $Z = 4$  for the formula unit,  $\text{C}_{27}\text{H}_{27}\text{F}_3\text{N}_2\text{O}_5$ . The final anisotropic full-matrix least-squares refinement on  $F^2$  with 335 variables converged at  $R1 = 4.26\%$ , for the observed data and  $wR2 = 14.04\%$  for all data. The goodness-of-fit was 1.032. The largest peak in the final difference electron density synthesis was  $0.289 \text{ e/\AA}^3$  and the largest hole was  $-0.257 \text{ e/\AA}^3$  with an RMS deviation of  $0.059 \text{ e/\AA}^3$ . On the basis of the final model, the calculated density was  $1.363 \text{ g/cm}^3$  and  $F(000)$ , 1080 e $^-$ .

## Acknowledgements

Authors thank supports from MINECO and FEDER (MAT2015-69367-R, MAT2015-69547-R and CTQ2013-40855-R) and Gobierno de Aragón - Fondo Social Europeo (research group E40). Support for the research of C.A. was received through the prize "ICREA Academia" for excellence in research funded by the Generalitat de Catalunya.

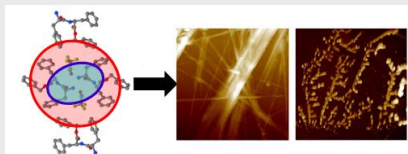
**Keywords:** Fibers; Hydrophilic core; Nanoplates; Peptide materials; Stacking interactions

- [1] M. Reches, E. Gazit, *Science* **2003**, *300*, 625–627.
- [2] P. Tamamis, L. Adler-Abramovich, M. Reches, K. Marshall, P. Sikorski, L. Serpell, E. Gazit, G. Archontis, *Biophys. J.* **2009**, *96*, 5020–5029.
- [3] C. H. Görbitz, *Chem. Commun.* **2006**, 2332–2334.
- [4] L. Adler-Abramovich, M. Reches, V. L. Sedman, S. Allen, S. J. B. Tendler, E. Gazit, *Langmuir* **2006**, *22*, 1313–1320.
- [5] M. Reches, E. Gazit, *Phys. Biol.* **2006**, *3*, S10–S19.
- [6] M. Reches, E. Gazit, *Nano Lett.* **2004**, *4*, 581–585.
- [7] E. Mayans, G. Ballano, J. Casanovas, A. Díaz, A. Pérez-Madrígal, F. Estrany, J. Puiggalí, C. Catiuela, C. Alemán, *Chem. Eur. J.* **2015**, *21*, 16895–16905.
- [8] X. Yan, J. Li, H. Möhwal, *Adv. Mater.* **2011**, *23*, 2796–2801.
- [9] J. Raeburn, A. Zamith Cardoso, D. J. Adams, *Chem. Soc. Rev.* **2013**, *42*, 5143–5156.
- [10] A. Mahler, M. Reches, M. Rechter, S. Cohen, E. Gazit, *Adv. Mater.* **2006**, *18*, 1365–1370.
- [11] N. Amdursky, R. Orbach, E. Gazit, D. Huppert, *J. Phys. Chem. C* **2009**, *113*, 19500–19505.
- [12] V. Jayawarna, M. Ali, T. A. Jowitt, A. F. Miller, A. Saiani, J. E. Gough, R. V. Ulijn, *Adv. Mater.* **2006**, *18*, 611–614.

- [13] A. M. Smith, R. J. Williams, C. Tang, P. Coppo, R. F. Collins, M. L. Turner, A. Saiani, R. V. Ulijn, *Adv. Mater.* **2008**, *20*, 37-41.
- [14] C. Tang, A. M. Smith, R. F. Collins, R. V. Ulijn, A. Saiani, *Langmuir* **2009**, *25*, 9447-9453.
- [15] M. Zhou, A. M. Smith, A. K. Das, N. W. Hodson, R. F. Collins, R. V. Ulijn, J. E. Gough, *Biomaterials* **2009**, *30*, 2523-2530.
- [16] J. Raeburn, G. Pont, L. Chen, Y. Cesbron, R. Levy, D. J. Adams, *Soft Matter* **2012**, *8*, 1168-1174.
- [17] N. A. Dudukovic, C. F. Zukoski, *Langmuir* **2014**, *30*, 4493-4500.
- [18] J. Raeburn, C. Mendoza-Cuenca, B. N. Cattoz, M. A. Little, A. E. Terry, A. Z. Cardoso, P. C. Griffiths, D. J. Adams, *Soft Matter* **2015**, *11*, 927-935.
- [19] V. Jayawarna, A. Smith, J. E. Gough, R. V. Ulijn, *Biochem. Soc. Trans.* **2007**, *35*, 535-537.
- [20] E. Mayans, G. Ballano, J. Casanovas, L. J. del Valle, M. M. Pérez-Madrugal, F. Estrany, A. I. Jiménez, J. Puiggalí, C. Cativiela, C. Alemán, *Soft Matter* **2016**, *12*, 5475-5488.
- [21] P. W. J. M. Frederix, R. Kania, J. A. Wright, D. A. Lamprou, R. Ulijn, C. J. Pickett, N. T. Hunt, *Dalton Trans.* **2012**, *41*, 13112-13119.
- [22] W. Helen, P. de Leonardis, R. V. Ulijn, J. Gough, N. Tirelli, *Soft Matter* **2011**, *7*, 1732-1740.
- [23] M. Zhou, A. M. Smith, A. K. Das, N. W. Hodson, R. F. Collins, R. V. Ulijn, J. E. Gough, *Biomaterials* **2009**, *30*, 2523-2530.
- [24] V. Jayawarna, S. M. Richardson, A. R. Hirst, N. W. Hodson, A. Saiani, J. E. Gough, R. V. Ulijn, *Acta Biomater.* **2009**, *5*, 934-943.
- [25] Y. Yamauchi, M. Yoshizawa, M. Fujita, *J. Am. Chem. Soc.* **2008**, *130*, 5832-5833.
- [26] K. V. Rao, S. J. George, *Chem. Eur. J.* **2012**, *18*, 14286-14291.
- [27] P. Zhu, X. Yan, S. Su, Y. Yang, J. Li, *Chem. Eur. J.* **2010**, *16*, 3176-3183.
- [28] R. Huang, W. Qi, R. Su, J. Zhao, Z. He, *Soft Matter* **2011**, *7*, 6418-6421.
- [29] P. Kumaraswamy, R. Lakshmanan, S. Sethuraman, U. M. Krishnan, *Soft Matter* **2011**, *7*, 2744-2754.
- [30] S. Bartocci, I. Morbioli, M. Maggini, M. Mba, *J. Pept. Sci.* **2015**, *21*, 871-878.
- [31] J. Wang, K. Liu, L. Yan, A. Wang, S. Bai, X. Yan, *ACS Nano* **2016**, *10*, 2138-2143.
- [32] T. H. Han, J. K. Oh, G.-J. Lee, S. I. Pyun, S. O. Kim, *Colloid Surf. Sci. B: Biointerfaces* **2010**, *79*, 440-445.
- [33] C. H. Gorbitz, *Chem. Eur. J.* **2001**, *7*, 5153-5159.
- [34] X. Yan, P. Zhu and J. Li, *Chem. Soc. Rev.* **2010**, *39*, 1877-1890.
- [35] V. Castelletto, J. E. McKendrick, I. W. Hamley, U. Olsson, C. Cenker, *Langmuir* **2010**, *26*, 11624-1162.
- [36] S. T. Kumar, J. Meinhardt, A. K. Fuchs, T. Aumüller, J. Leppert, B. Büchele, U. Knüpfer, R. Ramachandran, J. K. Yadav, E. Prell, I. Morgado, O. Ohlenschläger, U. Horn, T. Simmet, M. Görlach, M. Fändrich, *ACS Nano* **2012**, *8*, 11042-11052.

Entry for the Table of Contents (Please choose one layout)

ARTICLE



The assembly of a diphenylalanine amphiphile stabilized by a trifluoroacetate ion is regulated through the properties of solvents mixtures.

*Enric Mayans, Gema Ballano, Javier Sendros, Merçè Font-Bardia, J. Lourdes Campos, Jordi Puiggali,\* Carlos Cativiela,\* and Carlos Alemán\**

**Page No. – Page No.**

**Effect of the solvent choice in the self-assembly properties in a diphenylalanine amphiphile stabilized by an ion pair**